Multi-objective energy storage capacity optimisation considering Microgrid generation uncertainties

Multi-objective optimisation and planning of grid-connected cogeneration systems in presence of grid power fluctuations and energy storage dynamics

R. Garmabdari*, M. Moghimi, F. Yang, J. Lu

School of Engineering, Griffith University, Nathan Campus, Nathan, QLD 4111, Australia

ARTICLEINFO

Article history:
Received
Received in revised form

Keywords:
Cogeneration systems
Combined heat and power
CHP
Planning and sizing
Operation optimisation

ABSTRACT

In recent years, multi-generation systems (MGS) have been at the centre of attention for incorporating various energy sources and technologies to provide a reliable and sustainable energy supply. However, deciding on the most suitable configuration and optimal operation strategy of MGS has always been a challenging issue due to the nonlinear and complex interactions between different energy converters. Cogeneration solutions offer excellent energy efficiency through the coproduced heat from the electricity generation process. This will lead to significant economic profitability compared to conventional independent heat and power production plants. This paper presents a mixed-integer quadratic based multi-objective structural design strategy for grid-connected cogeneration systems comprising combined heat and power (CHP) devices, ancillary boiler, and energy storage devices in presence of nonlinear and dynamic behaviour of the energy storage systems. The power fluctuations smoothing index (PFSI) and energy storage depreciation factor (ESDF) are defined to effectively mitigate the power grid fluctuations and extend the lifetime of the energy storage systems. Presenting three case scenarios, the obtained results demonstrate the efficacy and applicability of the developed technique and reflect the impact of the introduced factors on the optimal configuration and operation of cogeneration systems.

1. Introduction

Conventional energy networks such as gas and electricity are traditionally implemented and operated independently. In addition to the adverse environmental impacts of conventional energy production methods, they suffer from low energy security, high operation cost, low energy efficiency, and low robustness [1–3].

In order to resolve the aforementioned issues, multi-generation plants consisting of several renewable resources and distributed electricity and heat generation units were introduced. The key feature of these systems is the potential capability of capturing the coproduced heat associated with electricity generation to satisfy the thermal or cooling demand, hence improving the sustainability of energy production. Deploying energy-efficient technologies in multi-generation systems (MGS) will ultimately lead to techno-economic and environmental benefits as well as energy supply security and efficiency improvement. Among various MGSs, cogeneration systems are effective and feasible solutions to harness the excess generated heat in commercial and residential buildings.

There are several determinative factors involved in selecting the technology and capacity of the equipment in a cogeneration system such as the abundance and availability of the resources, energy demand profiles, investment cost, technical specification and operating constraints of the energy converters [4–6].

* Corresponding author.
E-mail address: rasoul.garmabdari@Griffithuni.edu.au (R. Garmabdari).

Nomenclature

Abbreviations

AB	Ancillary Boiler
CCHP	Combined Cooling, Heating and Power System
CHP	Combined Heat and Power
CR	Capacity Rating
DOD	Depth of Discharge
DP	Dynamic Programming
ESDF	Energy Storage Degradation Factor
ESS	Energy Storage System
GA	Genetic Algorithm
MGS	Multi-generation System
MINLP	Mixed-Integer Linear Programming
MIQ	Mixed Integer Quadratic Model
MIQP	Mixed-Integer Quadratic Programming
PFSI	Power Fluctuation Smoothing Index
PR	Power Rating
RES	Renewable Energy Sources
SOC	State of Charge
TES	Thermal Energy Storage
UC	Unit Commitment

Indices

i	Energy storage technology
j	Energy conversion unit technology
r	Renewable energy source
t	Time
ϵ	Available technologies of CHP units
κ	Energy conversion unit number
λ	Available technologies of AB units
μ	Number of available AB
ω	Number of available CHP units

Subscripts

b	Battery storage system
cap	Capital
ch	Charging state of energy storage
dis	Discharging state of energy storage
e	Electricity generation
EC	Energy conversion unit
ESS	Energy storage system
exp	Export
G	Upstream grid-related parameter
g	Natural gas
h	Heat generation
imp	Import
$\mathcal{M}$	Maintenance
op	Operation
th	Thermal storage
tot	Total

Superscripts

sdn	Shutdown
stu	Startup
STR	Status transition
Max	Maximum
Min	Minimum

Latin symbols

AR	Available reserve
C	Cost
CR	Capacity rating decision variable
cp	Specific heat capacity
DOD	Depth of discharge of energy storage
dt	Time interval
$d\theta$	Temperature difference
E	Energy content of energy storage
ED	Electricity demand
$ESDF$	Energy storage degradation factor
F	Consumed fuel
HD	Heat demand
Ir	Interest rate
LT	Project lifetime
P	Power
$PFSI$	Grid power fluctuations smoothing index
PR	Power rating decision variable
RD	Ramp-down rate
RU	Ramp-up rate
SOC	Energy storage state of charge
T	Planning horizon
W	Weighting factor
x, y, z	Coefficients

Greek symbols

α	Fuel consumption coefficient
β	Loss coefficient
Γ	Energy storage power rating coefficient
γ	Boolean variable indicating installation status
ε	Small number
ζ	Boolean variable indicating commitment status
η	Efficiency
Λ	Continuous ancillary variable
Π	Large number
ρ	Density of energy storage medium
σ	Heat energy loss ratio
τ	Battery energy loss ratio
ϑ	Boolean decision variable
χ	Energy storage operating capacity coefficient
ψ	Component available reserve

Therefore, the optimal sizing of cogeneration systems necessitates establishing the techno-economic model of the components and the relationships between energy converters. Optimal coordination of energy converters within a system is of utmost significance as the operating cost of elements directly affects the total cost of the cogeneration system and hence its payback period over the long-term [5,7]. Furthermore, the architecture and coupling factors of units depend on the demand features, cost of energy wares, and techno-operational constraints of the components. A cogeneration system is basically composed of Combined Heat and Power (CHP) units and Ancillary Boilers (AB) as the primary and secondary energy converters and Energy Storage Systems (ESS).

Cogeneration systems are capable of operating in both stand-alone and grid-connected modes. The grid-connected system has increasingly become the centre of interest in recent years due to the high reliability, flexibility and security in supplying demand [8,9].

The performance of the cogeneration system is affected by the operational constraints and efficiency of the energy conversion units. The efficiency of an energy converter is a dynamic function of the temperature and output power at which the corresponding device is operating [10]. Moreover, the dynamic behaviour of the equipment, particularly ESS units, play a crucial role in optimal sizing of the components.

Another important factor that comes to attention when dealing with a grid-connected system in commercial and industrial cases is the power fluctuations of the upstream grid [11,12]. Since the utility companies are required to respond to the demand at any given time, therefore a peak demand for a short period urges the utility grid to dispatch more generation units that would impose a high cost on the network. To compensate for this excess cost, customers are charged for the gap between their average and peak demand value [13].

In the literature, abundant studies have been carried out on operation strategies and structural planning of cogeneration systems, taking the environmental, technical and economic aspects into account. In previous studies, authors have merely considered the technical and economic perspective associated with of sizing and optimal scheduling of cogeneration systems without taking the impact of ESS degradation and grid power variations into account [14–16].

In publication [17], authors introduced a multi-level optimisation approach, the first level of which evaluates all various possible configuration through evaluating a combined cost and energy utilisation objective function. The second and third level, on the other hand, assess the optimised configuration and apply modification where necessary.

This study focuses on the economic viability of the cogeneration system in a district heating network and hence considering a seasonal planning approach where the grid power variations, dynamic and nonlinear operation of elements in the system are overlooked. Refs [6,18–20] have mainly dealt with the existing uncertainties in electricity and gas dynamic pricing, the generation of renewables and energy demand, using probabilistic methods, while mitigating the CO2 emissions. Nonetheless, authors in [6,18,19] have not considered ESS in their structural optimisation model. Moreover, publication [20], not only ignored the impact of power fluctuation and BES degradation on the optimised solution but also employed a nonlinear model to solve the established planning problem. Authors in [21] have presented a two-layer framework using Dynamic Programming (DP) optimisation strategy for configuration design and operation of hybrid energy plants to simultaneously minimise the carbon emissions and total cost of the system. The first stage of the proposed method aims at maximising the economic profit and minimising the carbon emission over the lifetime of the project through selecting a random structure at minimum investment cost, whereas the second stage focuses on the optimal scheduling of the equipment with the objective of operating cost reduction. Similarly, papers [22,23] adapted Genetic Algorithm (GA) and Mixed-Integer Nonlinear Programming (MINLP) as the inner and outer layers of the proposed two-stage cooptimisation technique to determine the most proper size of the components and optimal operation of the system. Paper [24] opted a similar approach with an emphasis on net zero emission constraint as the environmental factor and demand response to determining the size and type of the components. However, in none of the above articles, the mitigation of the power variations and degradation effect of BES are taken into account. Furthermore, employing a nonlinear modelling approach would result in computational complexity and longer convergence time.

On the other hand, publication [25] proposed a robust optimisation method to optimally integrate various energy wares, considering the intermittency of renewable energies. Furthermore, paper [26] inspected the degree of impact of climate at the location of trigeneration systems so-called Combined Cooling, Heating and Power (CCHP) systems, on the size and choice of components through analysing different scenarios to address the optimal element sizing problem. The equipment selection is based on minimising the objective function which solely considers the energy consumption cost. A similar approach was developed in [27,28] to optimally schedule the operation of the components within a distributed network with the aim of operation cost and environmental minimisation. The nonlinear transmission constraint of natural gas is approximated by a linear piecewise function to turn the MINLP into a linear form. However, no energy storage is included in the investigated structure. Authors in publications [29] addressed the optimal selection and capacity of energy converters, considering the reliability of supply as well as cost minimisation. Researchers in [30,31] developed a sizing and placement algorithm in which the operation and investment cost of cogeneration systems are minimised in a distributed system. The costs associated with power losses, voltage profile, and energy outage, as well as their related constraints, are included in the optimisation model. Paper [32] has reported a multi-criterion fuzzy-based decision-making approach to deal with the complexity of selecting the proper configuration out of the energy source pool, considering the ecological and environmental impacts. However, the authors merely inspected the choice of the technology of energy sources rather than the detailed components' specifications.

On the other hand, several research papers have focused on the optimal dispatching of energy converters in a cogeneration system, considering the economical or environmental aspects [33–36]. The authors in [34] proposed an operational model for CCHP units, taking the demand response and dynamic operation of the energy storage into account. Nevertheless, the variable operating cost of energy storage and variable maintenance cost of conversion units have been neglected. The researchers in [37] propose a unit-commitment based approach to optimally schedule a multi-energy conversion system in incorporation with energy storage.

To address the shortcomings of the previous studies, this paper presents a multi-objective optimisation framework to simultaneously obtain the most techno-economical architecture as

well as the operation strategy of cogeneration systems. A thermal and battery energy storage to facilitate the grid integration and enhance the penetration of renewables are included in the configuration that their optimal capacity and power rating are to be achieved. To this end, the proposed model takes the dynamic behaviour of the energy storage devices, the depreciation cost and the operating criteria of the energy converters into account. Furthermore, the grid power fluctuations, as well as the degradation of BES, are effectively reduced through introducing Power Fluctuation Smoothing Index (PFSI) and Energy Storage Degradation Factor (ESDF). The primary aim of this method is to effectively lessen the investment cost while fulfilling the operating criteria and improving the performance of the cogeneration system. To achieve this, a new Mixed-Integer Quadratic (MIQ) model is developed to address the optimal dispatch problem and structural design problem with a second-order multi-objective function subjected to a set of nonlinear and complex operation and sizing criteria that are linearised to avoid computational complexity.

The rest of this paper is organised in four sections as follows: In the second section, the architecture of the understudy cogeneration system is described in detail. Furthermore, a generic mathematical model, as well as operational constraints of the components, are developed. In section 3, the objective function subjected to the established constraints in section 3 is derived. Section 4 investigates three different case studies to verify the effectiveness and applicability of the proposed approach. Furthermore, the impact of introduced objective terms is inspected by performing sensitivity analysis. Lastly, section 5 concludes the paper.

2. Cogeneration System Architecture

Although incorporating various energy carriers at the input enables the energy conversion devices to cover the inherent shortcomings of one another [9], this integration of electricity and heat energy converters results in the interdependency of the conversion units. This interaction significantly affects the optimal operation of the cogeneration unit and its economic viability, which subsequently will have a great impact on the optimal capacity of the components. The elements utilised in cogeneration systems can be classified into three main types; direct energy supply from an upstream grid, converters, and energy storage devices [38]. Converter devices are used to transform the energy or energy carriers to the required form of energy such as gas boilers, heat pump, and gas turbines.

On the other hand, energy storage systems are employed to store the excess produced energy and dispatch it during the peak demand period to effectively reduce the energy consumption cost [1,2,12]. However, owing to their high investment cost and short lifetime compared to other conversion units, oversizing or under-sizing of these elements will reduce the economic profitability of the cogeneration system. Hence, optimal size determination of these components is very paramount in the planning and operation of cogeneration systems.

As demonstrated in Fig. 1, the understudy system is a hybrid grid-tied cogeneration system encompassing renewable generation units, CHP generators, battery and Thermal Energy Storage (TES) units, and upstream grid connection. This system utilises the cogenerated heat from n units of CHP generators, the heat produced by m units of AB, and the discharged heat from the thermal storage to satisfy the heat demand. The electrical load, however, is supplied by the imported electricity from the grid, electricity produced by renewable resources generated electricity from CHP units, and discharged power of battery storage.

3. Generic Operating Model of Cogeneration System

Determining the type and optimal capacity of the elements from a range of available technologies entails establishing the operating model of the candidate elements as well as developing the relationship between the energy carriers at the inputs and energy demands at the outputs of the system.

3.1. Energy conversion units

The output power of the CHP units is determined through the following equations where $\eta_{CHP,e}$ and $\eta_{CHP,h}$ are respectively the electricity and heat conversion efficiencies.

$$P_{CHP,e}^{\epsilon,\omega}(t) = \gamma_{\epsilon,\omega} \times \eta_{CHP,e} \times \alpha_{\epsilon,\omega}(t) \times \mathrm{F}_{tot}(t) \quad (1)$$

$$P_{CHP,h}^{\epsilon,\omega}(t) = \gamma_{\epsilon,\omega} \times \eta_{CHP,h} \times \alpha_{\epsilon,\omega}(t) \times \mathrm{F}_{tot}(t) \quad (2)$$

where $P_{CHP,e}(t)$, $P_{CHP,h}(t)$ denote the electricity and heat generated by the CHP unit. ϵ, ω, $\alpha(t)$, and F_{tot} represent available technologies of CHP, the total number of available CHP units to be installed, fuel consumption coefficient, and the total amount of consumed fuel, respectively. γ is defined as a set of binary variables, indicating the installation status of the candidate elements. The temperature of hot water demand for domestic use is assumed to be around 50º, this temperature can be regulated by mixing cold water with the hot water [6]. In this study, the heat demand implicates the thermal energy required by the building so that the hot water and space heating is always delivered at a sufficiently high temperature by utilising actual CHP components.

Similarly, the output power of the AB, $P_{AB}(t)$, is defined as a function of the fuel it consumes at instant t as formulated below:

$$P_{AB}^{\lambda,\mu}(t) = \gamma_{\lambda,\mu} \times \eta_{AB} \times \alpha_{\lambda,\mu}(t) \times \mathrm{F}_{tot}(t) \quad (3)$$

where λ and μ are available technologies of AB, and the total

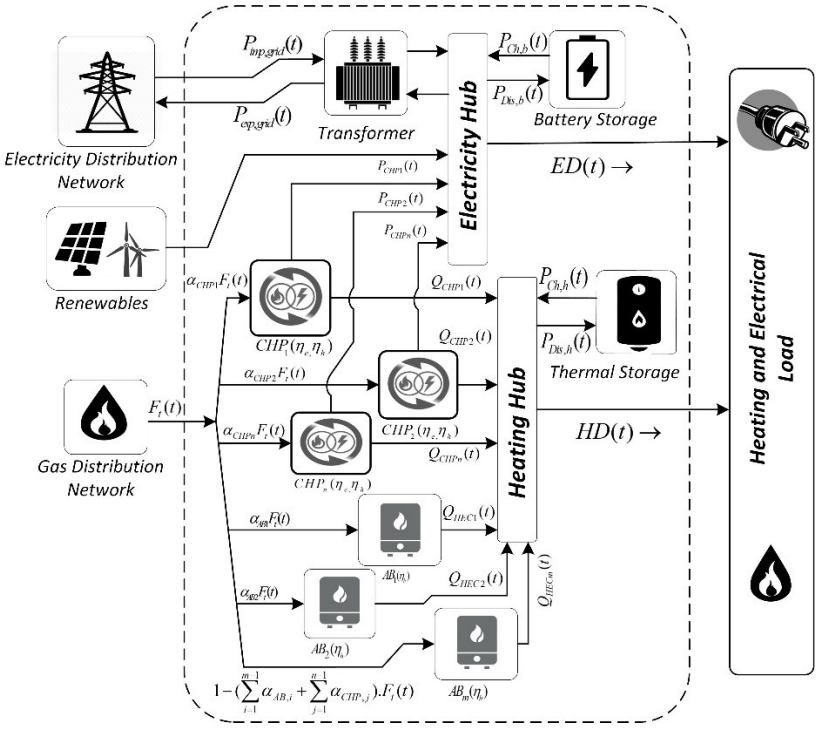

Figure 1. The structure of the understudy cogeneration system.

number of available AB units to be installed.

Regardless of the technology of the energy converters, their operational model involves expressing several technical parameters including ramp rate limits, upper and lower output power bounds.

Since the installed units of the same type are operating in a parallel configuration, increasing the number of units linearly increases the ramp rates and output power capacity limits of the corresponding unit. Therefore, the maximum and minimum power of j-type unit, which are respectively denoted by P_j^{Min} and P_j^{Max}, can be determined using Eq. (4).

$$P_j^{Min} \times \sum_{\kappa_j} \gamma_{j,\kappa} \leq P_j(t) \leq P_j^{Max} \times \sum_{\kappa_j} \gamma_{j,\kappa} \tag{4}$$

where $\gamma_{j,k}$ and $P_j(t)$ are the installation indicator variable of the κ^{th} unit of type j and output power of unit j at the time instant t.

On the other hand, to constrain the ramp rates of the units, installation and commitment status variables of the energy converters should be both equal to one for an increase in the ramp limit of unit j.

For instance, if K number of units of type j are installed, but only a few of them are operating at instant t, then the ramps limits would be equal to the sum of ramp limit values of the activated elements. This statement can be formulated as in Eq. (5).

$$\sum_{\kappa_j} \zeta_{j,\kappa}(t) \times \gamma_{j,\kappa} \times RD_j \leq P_j(t) - P_j(t-1) \leq \sum_{\kappa_j} \zeta_{j,\kappa}(t) \times \gamma_{j,\kappa} \times RU_j \tag{5}$$

where RU_j and RD_j are the ramp-up and ramp-down rates of particular unit j. The decision variable $\zeta_{j,k}(t)$ represents the commitment status of κ^{th} unit of type j at time t that will be further explained in section 4.

3.2. Energy storage system model

The operation of the BES device is described by a dynamic model through which the stored energy in the storage device at any given interval is calculated as expressed in Eq. (6).

$$E_{ESS,b}(t) = E_{ESS,b}(t-1) \times (1-\tau) + \left(P_{ch,b}(t) \times \eta_{ch,b} - \frac{P_{dis,b}(t)}{\eta_{dis,b}}\right) \times dt \tag{6}$$

where $E_{ESS,b}(t)$, $\eta_{ch,b}$, and $\eta_{dis,b}$ represent the amount of energy left in the storage, charging efficiency, and discharging efficiency of the BES, respectively. τ denotes the energy loss ratio which is negligible for BES compared to that of TES.

The energy content of TES is expressed using a dynamic

function which is similar to that of BES as describe in equation Eq. (7).

$$E_{ESS,th}(t) = E_{ESS,th}(t-1) \times (1-\sigma) + \left(P_{ch,th}(t) \times \eta_{ch,th} - \frac{P_{dis,th}(t)}{\eta_{dis,th}}\right) \times dt \quad (7)$$

where $E_{ESS,h}(t)$, $\eta_{ch,h}$, $\eta_{dis,h}$, and σ represent energy content, charging efficiency, discharging efficiency, and energy loss ratio of the TES, respectively.

The energy loss coefficient of the thermal storage which has a relationship with the capacity of the thermal storage has a significant impact on the instantaneous energy level of the thermal storage. The heat loss coefficient of the thermal storage is defined as the amount of heat that is lost within a certain period and is directly correlated with the medium employed in the storage, the difference of storage surrounding, and medium temperature [39] as described in Eq. (8).

$$\sigma = \sigma_0 \times \sqrt{\left(\frac{CR_{ESS,th}}{cp \times \rho \times d\theta}\right)^3} \quad (8)$$

where $CR_{ESS,th}$, cp, ρ, and $d\theta$ are receptively the nominal capacity of thermal storage, specific heat, the density of the medium, and temperature difference. Assuming that the temperature difference, $d\theta$, is maintained at a constant value, the above nonlinear equation can be approximated by a second-order polynomial function as shown in the following equation where the loss coefficients x, y, and z are calculated according to the specific heat and density of the medium as well as the temperature difference.

$$\sigma_{ESS,h} = x \times \left(CR_{ESS,th}\right)^2 + y \times CR_{ESS,th} + z \quad (9)$$

In addition to the dynamic energy model, the energy level in the storage devices has to be between the maximum depth of discharge and the total capacity of the energy storage at any given interval. Furthermore, the charge and discharge rates should be constrained within a certain range. As the charging and discharging events cannot occur simultaneously, a binary variable ($\vartheta_{Ess,i}(t)$) needs to be defined to ensure that the energy storage is either in charging or discharging mode.

Nevertheless, since the capacity and power rating of the energy storage are two decision variables, the charge and discharge power limits that are unknown should be related to these variables. To establish this correlation, the proposed constraints from Eq. (10) to Eq. (12) must be satisfied.

$$P_{ch,i}(t) - \left(\vartheta_{Ess,i}(t) \times \Gamma_{ch,i}^{Max} \times PR_{ESS,i}\right) \leq 0 \quad (10)$$

$$P_{dis,i}(t) - \left(\left(\vartheta_{Ess,i}(t) - 1\right) \times \Gamma_{dis,i}^{Max} \times PR_{ESS,i}\right) \quad (11)$$

$$\left(\Gamma_{ch,i}^{Max}, \Gamma_{dis,i}^{Max}\right) \in \{0 \dots 1\}$$

$$P_{ESS,i}^{Min} \leq PR_{ESS,i} \leq P_{ESS,i}^{Max} \quad (12)$$

where $P_{ESS,i}^{Max}$, and $P_{ESS,i}^{Min}$the maximum and minimum values of the design parameter for the power rating of energy storage of type i ($PR_{ESS,i}$). The maximum and minimum values of the design parameters for the energy storage are determined based on available physical space or other unforeseen circumstances that might limit the physical installation of the energy storage. $\Gamma_{ch,i}^{Max}$, $\Gamma_{dis,i}^{Max}$ imply the upper bound power range coefficients for charging and discharging rate of the energy storage and are expressed as a fraction of unity. The power range coefficients define the relationship between the maximum charge/discharge power rating of the energy storage to the determined nominal power of the battery ($PR_{ESS,i}$). For instance, if the power rating of the energy storage is equal to P value and the upper bound power coefficient for charging, $\Gamma_{ch,i}^{Max}$, is equal to 0.5, then the maximum charging power cannot exceed $\frac{1}{2}P$. The same concept applies to the upper bound power coefficient for discharging ($\Gamma_{dis,i}^{Max}$) and the design parameter $PR_{ESS,i}$ to infer the maximum discharge power rate of the energy storage i as expressed in Eq. (11).

Nevertheless, the multiplication of the binary charge/discharge status variable ($\vartheta_{Ess,i}(t)$) and the power rating design variable, $PR_{ESS,i}$, in Eqs. (10) and (11) turns the sizing problem into a nonlinear optimisation problem. To avoid this, the equivalent linear constraints of these multiplications is developed by adding a new set of continuous variables, $\Lambda_{ESS,i}(t)$, as stated in Eq. (13) to Eq. (16).

$$P_{ESS,i}^{Min} \times \vartheta_{Ess,i}(t) \leq \Lambda_{ESS,i}(t) \leq P_{ESS,i}^{Max} \times \vartheta_{Ess,i}(t) \quad (13)$$

$$PR_{ESS,i} - \left(1 - \vartheta_{Ess,i}(t)\right) \times P_{ESS,i}^{Max} \leq \Lambda_{ESS,i}(t) \quad (14)$$

$$PR_{ESS,i} + P_{ESS,i}^{Min} \times \left(1 - \vartheta_{Ess,i}(t)\right) \leq -\Lambda_{ESS,i}(t) \quad (15)$$

$$PR_{ESS,i} - P_{ESS,i}^{Max} \times \left(1 - \vartheta_{Ess,i}(t)\right) \leq -\Lambda_{ESS,i}(t) \quad (16)$$

In addition to the limitations on the power of energy storage, its energy level should be confined to the lower and upper limits. As this range varies according to the optimal capacity rating of the energy storage ($CR_{ESS,i}$), a maximum operating capacity coefficient is introduced to the model. This new variable is selected between zero and one and its relationship with the capacity design parameter ($CR_{ESS,i}$) is defined as a linear constraint, as shown in Eq. (17).

$$(1 - DOD_i) \times CR_{ESS,i} \le E_{ESS,i}(t) \le \Gamma_{ESS,i} \times CR_{ESS,i}$$
$$\Gamma_{ESS,i} \in \{0 \dots 1\} \quad (17)$$

DOD and $\Gamma_{ESS,i}$ represent the depth of discharge of the energy storage and maximum operating capacity coefficient, which is selected within zero and one.

3.3. Energy flow balance

The aggregation point of the energy flows that involves the energy conversion units and energy storage devices is referred to as an energy hub as depicted in Fig. 1. To ensure that the installed components satisfy the heat and electricity demands over the planning horizon, the generation-demand balance at each energy hub must hold at every time interval.

$$\begin{aligned} P_{ch,b}(t) + ED(t) + P_{exp}(t) &= P_{dis,b}(t) + \sum_{r} P^{r}_{RES}(t) \\ &+ \sum_{\epsilon}\sum_{\omega} \zeta_{\epsilon,\omega}(t) \times P^{\epsilon,\omega}_{CHP,e}(t) \times \gamma_{\epsilon,\omega} \\ &+ P_{imp}(t) \end{aligned} \quad (18)$$

$$\begin{aligned} P_{ch,th}(t) + HD(t) &= P_{dis,th}(t) \\ &+ \sum_{\lambda}\sum_{\mu} \zeta_{\lambda,\mu}(t) \times P^{\lambda,\mu}_{AB}(t) \times \gamma_{\lambda,\mu} \\ &+ \sum_{\epsilon}\sum_{\omega} \zeta_{\epsilon,\omega}(t) \times P^{\epsilon,\omega}_{CHP,h}(t) \times \gamma_{\epsilon,\omega} \end{aligned} \quad (19)$$

$$\{\lambda, \epsilon\} \subset j$$
$$\{\mu, \omega\} \subset k_j$$

where $P^{r}_{RES}(t)$, $ED(t)$, and $HD(t)$ imply the generated electricity by r^{th} RES, electricity demand, and heat demand at time instant t.

Besides the energy balance, the amount of gas fuel purchased from the distribution network is limited. To include this limitation in the model, the following constraint should be satisfied:

$$0 \le \mathrm{F}_{tot}(t) \le \mathrm{F}^{Max}_{tot} \quad (20)$$

3.4. Available reserve and utility grid constraints

The loads connected to the cogeneration system are categorised into two types: critical loads that require continuous and reliable supply and non-critical loads. In order to ensure that the system is capable of meeting the critical loads in case of sudden changes in demand, the available reserve constraints are imposed while determining the optimal size of components. The available reserve, denoted by $AR_n(t)$ for energy hub n, is defined as the maximum level of deliverable energy during each interval and is computed by aggregation of the difference between the maximum capacity of the operating devices and their corresponding generated power at instant t as formulated in Eq. (21).

$$\begin{aligned} \sum_{j} Min\{K_j \times RU_j, \left(\kappa_j \times P^{Max}_{j} - \sum_{\kappa} P_{j,k}(t)\right) \\ + Min\{P^{Max}_{ESS,i}, E_{ESS,i}(t)\} \ge AR_n(t) \end{aligned} \quad (21)$$

The above inequality applies to both electricity and heating hubs and it only includes the components contributing to supplying the demand requirement corresponding to the relevant hub. However, the developed constraint in Eq. (21) contains Min-function that leads to nonlinearity in the model. In order to overcome this challenge, a set of continuous decision variables and linear inequalities corresponding to each component are defined to calculate the available reserve value for each unit at each time step. The inequalities Eq. (22) to Eq. (25) guarantee that the corresponding available reserve variables do not exceed the maximum ramp-up and nominal capacity of the units at each time step. Similarly, these conditions are applied to the energy storage components. The available reserve values for the energy storage devices are limited to the maximum discharge power and the instant energy content of the corresponding storage unit.

$$\psi_{j,k}(t) \le P^{Max}_{j}(t) \times \gamma_{j,k} \quad (22)$$

$$\psi_{j,k}(t) \le RU_j \times \gamma_{j,k} \quad (23)$$

$$\psi_{ESS,i}(t) \le \Gamma^{Max}_{dis,i} \times PR_{ESS,i} \quad (24)$$

$$\psi_{ESS,i}(t) \le E_{ESS,i}(t) \quad (25)$$

where $\psi_{j,k}(t)$, and $\psi_{ESS,i}(t)$ are respectively the available reserve values for the κ^{th} unit of type j, and energy storage device of type i at time t.

Adding the above constraints, the nonlinear available reserve inequality described in Eq. (21) is replaced with Eq. (26) and Eq. (27) for power and heating hubs, respectively.

$$\sum_{\epsilon}\sum_{\omega} \psi^{\epsilon,\omega}_{CHP,e}(t) + \psi_{BES}(t) \ge AR_e(t) \quad (26)$$

$$\sum_{\lambda}\sum_{\mu} \psi^{\lambda,\mu}_{AB}(t) + \sum_{\epsilon}\sum_{\omega} \psi^{\lambda,\mu}_{CHP,h}(t) + \psi_{TES}(t) \ge AR_h(t) \quad (27)$$

In addition to the operational constraints, the instant power exchanged with the grid should be constrained as represented in Eqs. (28) and (29).

$$0 \le P_{imp}(t) \le P_{imp}^{Max} \times \vartheta_G(t) \quad (28)$$

$$0 \le P_{exp}(t) \le \left(1 - \vartheta_G(t)\right) \times P_{exp}^{Max} \quad (29)$$

where P_{imp}^{Max} and P_{exp}^{Max} imply the upper bounds for importing and exporting power. Since simultaneous import and export of power from or to the grid is practically infeasible, a binary variable, $\vartheta_G(t)$, is included in the model to avoid this event.

4. Optimisation Model

4.1. Objective Function

The aim of the cogeneration system planning optimisation problem is to determine the size of the components, which results in minimum total cost (C_{tot}). The total cost includes two main elements: the investment cost and operation cost (C_{op}). A planning optimisation problem aims at selecting the most proper components from a pool of candidate devices to form the optimal configuration of the cogeneration system. The selection process and structure determination are performed based on the energy demand features, technical characteristics of the energy converters, and their corresponding capital and operation costs. Therefore, it is necessary to model all the available components in the pool and specify the limitations of the energy carriers. In order to represent the installation status of each component, a binary variable is assigned to each element in the pool as described in section 3. The objective function of the cogeneration system component sizing optimisation problem can be expressed as in Eq. (30).

$$Minimise\{C_{tot} = C_{cap,tot} \times \left(\frac{Ir \times (1+Ir)^{LT}}{(1+Ir)^{LT} - 1}\right) + C_{op}\} \quad (30)$$

where the $C_{cap,tot}$ denotes the total capital cost of the components including the conversion and storage units. The mathematical expression in the parenthesis in Eq. (30) represents the capital recovery factor which is defined as the uniform amount is to be paid annually over the lifespan (LT) of the project at the discount rate Ir.

4.2. Capital Cost Model

The capital cost of components comprises two main cost elements: the capital cost of the energy conversion units and energy storage devices as described in Eq. (31). The capital cost of the energy converters is calculated per unit and nonlinearly increases by the size and technology of the selected devices while the capital cost of the energy storage devices is a linear function of their size as shown in Eq. (31) and Eq. (32).

$$C_{cap,tot} = \sum_j \sum_{\kappa_j} C_{cap,j} \times \gamma_{j,\kappa} + \sum_i C_{cap,i} \times \gamma_i \quad (31)$$

where the $C_{cap,i}$, γ_i, and $C_{cap,j}$ denote the capital cost of energy storage of type i, installation indicator variable of storage i, and capital cost of energy converter of type j, respectively.

The capital cost of energy storage devices is computed according to their energy capacity and charge/discharge power rating as expressed in Eq. (32).

$$C_{cap,i} = C_{CR,i} \times CR_{ESS,i} + C_{PR,i} \times PR_{ESS,i} \quad (32)$$

where $C_{CR,i}$, $C_{PR,i}$ respectively represent capacity rating cost in \$/kWh, the capacity, power rating cost in \$/kW of the i^{th} energy storage device.

4.3. Operating Cost Model

The operating cost is regarded as a dynamic nonlinear function due to its dependency on different parameters including the demand profile, maintenance cost, efficiency, and fuel cost of the components. This nonlinear nature of structural planning and economic dispatch of cogeneration systems enhances the complexity and prolong the computing time of the optimisation problem. To avoid this, a Mixed Integer Quadratic Programming (MIQP) approach with linear constraints is proposed in this paper. In order to minimise the operating cost over the planning horizon, the economic dispatch and unit commitment (UC) problem is formed to perform power flow optimisation on the candidate cogeneration system configurations at each iteration of the algorithm.

The operating cost is composed of several elements including the cost associated with energy exchanged with the utility grid, cost of gas purchased from the network, maintenance cost, and status transition cost of energy converters as expressed in Eq. (33).

$$C_{op} = \sum_t \Bigg\{ \left[C_{G,imp}(t) \times P_{imp}(t) - C_{G,exp}(t) \times P_{exp}(t)\right] \times dt + \sum_i \left(C_{EC,tot}(t)\right) + ESDF \Bigg\} + PFSI \quad (33)$$

where $C_{G,imp}(t)$, $C_{G,exp}(t)$, $P_{imp}(t)$, $P_{exp}(t)$, and $C_{EC,tot}$ are the import electricity price, exported electricity price, imported power, exported power, and total operation cost of energy converters during dt interval. The last two terms in Eq. Eq. (33) are the grid power fluctuations smoothing index ($PFSI$) and energy storage degradation factor ($ESDF$), respectively.

4.4. Grid power fluctuations smoothing index (PFSI)

The grid power fluctuations, as described in section 1, impose an additional cost on the consumers. To mitigate these variations, the range of grid power fluctuation needs to be quantified. To address this issue, the PFSI is defined as a quadratic function that reflects the deviation of the imported power from its average value over the planning horizon as formulated in Eq. (34). Minimising this index regulates the grid variations, resulting in a more stable demand and lower operating cost. Since the imported power at each time instant is a decision variable in the cogeneration system component sizing problem, the PFSI can be considered either as a constraint or a term in the objective function of the optimisation problem. In this study, however, it is defined as an objective function as expressed in Eq. (34) and combined with operating cost and capital cost objectives.

$$PFSI = \left[\sum_{t}\left(P_{imp}(t) - \frac{1}{T}\sum_{t} P_{imp}(t)\right)^2\right] \times W_{PFSI} \tag{34}$$

where W_{PFSI} represents the power fluctuation cost coefficient, which should be proportionally assigned. Including this index in the objective function establishes a trade-off between the variation range of the grid power and the size of the components. Alternatively, the PFSI can be modelled as a constraint in the unit commitment and economic dispatch optimisation problem to sustain the grid power variations within certain limits.

4.5. Energy storage degradation factor (ESDF)

As described in section 1, even though the energy storage devices are the key components in cogeneration systems due to their significant contribution to reducing the energy demand and improving the PFSI, their extensive operation would exponentially reduce their lifetime. In order to avoid the excessive and instant fluctuations in the energy level of the storage units, the ESDF is introduced to the objective function.

The degradation of the energy storage devices is proportional to the amount of power flowing in or out of the device, the state of charge (SOC) level at instant t. A low SOC level reduces the lifetime of the energy storage significantly as explained in [40] in detail. Therefore, to minimise the depreciation of energy storage units, the ESDF is defined as a quadratic function of charge and discharge power with respect to the maximum power rating and the minimum SOC level of ESS over the planning horizon as described in Eq. (35).

$$ESDF = C_{ESS,b} \times \left(\frac{P_{ch,b}(t)^2}{P_{ch}^{Max}} + \frac{P_{dis,b}(t)^2}{P_{dis}^{Max}}\right) + \min_{T} SOC_b \times C_{SOC,b} \tag{35}$$

$P_{ch,b}(t)$, $P_{dis,b}(t)$, and $C_{SOC,b}$ are the charging power, discharging power, and cost coefficient related to the SOC level of the battery storage. $C_{ESS,b}$ represents the associated coefficient with the power flowing in and out of the BES.

4.6. Energy conversion unit cost model

To model the dynamic operation of energy converters, maintenance, and fuel cost of the candidate components should be taken into consideration. The total cost attributed to the operation of energy converters, represented by $C_{EC,tot}$ in Eq. (33) can be expressed as follows:

$$C_{EC,tot} = \sum_{j}\sum_{\kappa_j}\left(\left[\alpha_{j,k}(t) \times \mathrm{F}_{tot}(t) \times C_{\mathscr{g}}(t) + C_{\mathcal{M},tot} + \phi_{j,k}^{STR}(t)\right] \times \gamma_{j,k}\right) \tag{36}$$

where $\mathrm{C}_{\mathscr{g}}(t)$, $\alpha_{j,k}(t)$, and $\phi_{j,k}^{STR}(t)$ are the natural gas price, fuel consumption coefficient of the k^{th} unit of type j, and status transition cost, respectively.

The total maintenance cost of the energy converters at time slot t, denoted by $C_{\mathcal{M},tot}$, can be described as a dynamic function of its output power, as formulated follows:

$$C_{\mathcal{M},tot}(t) = \sum_{j}\sum_{\kappa_j}\left(\left(\gamma_{j,k} \times \alpha_{j,\kappa}(t) \times \mathrm{F}_{tot}(t) \times \eta_j\right) \times C_{\mathcal{M},j}\right) \times dt \tag{37}$$

where η_j and $C_{\mathcal{M},j}$ imply the efficiency and maintenance cost of the component of type j.

Changing the commitment status of a conversion unit imposes an additional operating cost on the system. This is caused by thermal and mechanical limitations, which extends the starting up and shutting down process duration. Therefore, to minimise the total operation cost, it is required to consider this cost component in the objective function as described in Eq. (38). For this purpose, a set of auxiliary binary variables (ζ) representing the commitment status of the energy conversion units are introduced to identify the transition status of the units over two consecutive time instants.

$$\phi_{j,k}^{STR}(t) = \left(C_j^{stu} \times \left(1 - \zeta_{j,\kappa}(t-1)\right) \times \zeta_{j,\kappa}(t) + C_j^{sdn} \times \left(1 - \zeta_{j,\kappa}(t)\right) \times \zeta_{j,\kappa}(t-1)\right) \times \gamma_{j,\kappa} \tag{38}$$

where C_j^{stu} and C_j^{sdn} are the startup and shutdown costs of the particular unit j. Defining the commitment status variables, the relationship between these variables and the unit installation status variables must be established. This correlation can be expressed as a conditional constraint so that if only one of the variables in the commitment status variable set for a unit is set to 1 over the entire planning horizon, the installation status of the corresponding unit

should be set to 1, as shown below:

$$\gamma_{j,\kappa} = \begin{cases} 1 & \sum_t \zeta_{j,\kappa}(t) > 0 \\ 0 & otherwise \end{cases} \quad (39)$$

To implement the aforementioned conditional statement in the MIQP, it needs to be converted into a series of linear constraints. As both installation ($\gamma_{j,\kappa}$) and commitment status ($\zeta_{j,\kappa}$) variables are binary, the following constraints are proposed to linearise this conditional statement.

$$\sum_t \zeta_{j,\kappa}(t) \geq 1 - \Pi \times (1 - \gamma_{j,\kappa}) \quad (40)$$

$$\sum_t \zeta_{j,\kappa}(t) \leq 1 - \varepsilon + (\Pi \times \gamma_{j,\kappa}) \quad (41)$$

where ε is selected as a fraction of 1, whereas Π is greater than the total number of available units to ensure that the model is able to handle the conditional statement stated in Eq. (39).

5. Simulation Results and Numerical Analysis

The developed MIQP optimisation model is implemented in the Matlab platform and solved using the CPLEX solver package. In this study, the proposed framework converts the naturally nonlinear functions, namely, maximum and minimum of a subset of decision variables, into linear functions using linear implementation techniques. The linear implementation techniques express the nonlinearities in the form of linear equations to avoid employing nonlinear programming methods that are time-consuming and complex to solve. In other words, the nonlinear functions are linearly described through introducing several linear equations and sets of auxiliary binary or continues variables. The linear implementation techniques do not create any errors in the results. However, there is another linearisation technique, so-called linear approximation, for converting single-variable nonlinear functions into linear functions. The linear approximation techniques may lead to small errors that are negligible and will not impact the optimality of the solution as investigated in [41].

The optimal size of the components of the understudy cogeneration system is obtained for three different case studies to evaluate the applicability and performance of the proposed method. Furthermore, the impact of the introduced parameters on the optimal solution is investigated by defining three case scenarios as tabulated below.

Table 1. Case studies defined for investigation of the proposed cogeneration system sizing approach

Case Scenarios	ESDF Included	PFSI Included
CASE A	No	No
CASE B	No	Yes
CASE C	Yes	Yes

The first case scenario optimises the capacity and configuration of the cogeneration system in which neither the ESS degradation factor nor the grid power fluctuations index is considered in the model. Case B, however, is designed to realise the significance of grid fluctuations in the grid-connected cogeneration system by considering the PFSI. In case C, the ESDF is included in the developed optimisation model to evaluate the impact of ESS degradation on both optimal structure and operation of the cogeneration system.

The understudy cogeneration system consists of electricity and heating hubs. The energy carriers, including natural gas, electricity imported from the grid, and renewable sources must satisfy the thermal and electricity demands. The energy converters utilised in the system are assumed to be CHP units and gas boilers. The type and number of available candidates and their corresponding installation costs considered in this study are listed in Table 2. In addition to the monetary aspect of the available units, their technical characteristics play a determinative role in the optimal sizing and operation of the cogeneration system. As shown in Table 2, these technical characteristics that confine the operation of the components directly affect the optimal solution of unit commitment problem, and consequently the operating cost.

In order to improve the economic viability of the cogeneration system, thermal storage linking to the heating hub and battery storage connected to the electricity hubs are utilised. The economic and technical characteristics of the candidate energy storage device are illustrated in Table 3. In this table, the power rating (PR) and capacity rating (CR) costs are provided per kW and kWh units, receptively.

The proposed approach optimises the nominal capacity and power rating of the ESSs as well as the technology and number of required energy converters that can meet the thermal and electrical load requirements at minimum cost. To realise the impact of individual factors on the optimal configuration of the cogeneration system, the same number of elements and characteristics are considered in all the defined case studies.

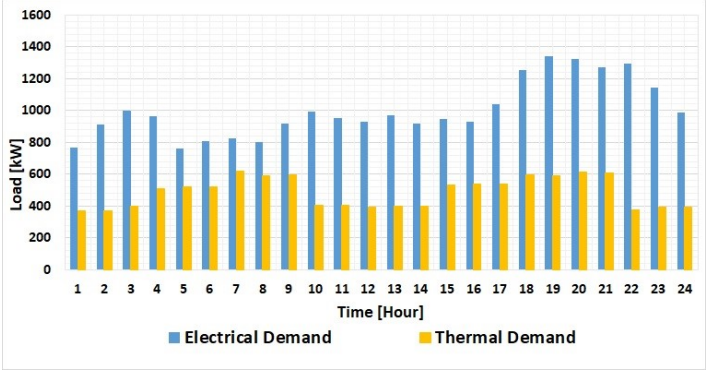

Figure 2. Electrical and thermal demands over the course of a day

Table 2. Economic and technical specifications of the candidate components

Description/Component	CHP type A	CHP type B	Boiler type A	Boiler type B	Unit
Available units	5	5	5	5	-
η_e	35	37	-	-	%
η_h	40	38	75	82	%
Max. Power	500	600	300	450	kW
Max. RU /RD	120	150	240	350	$\frac{kW}{h}$
Installation Cost	221000	237200	75000	100000	$

Table 3. Energy storage rated costs and their operating properties

ESS type	PR Cost [$\frac{\$}{kW}$]	CR Cost [$\frac{\$}{kWh}$]	Charge/Discharge Efficiency [%]	Min. DOD [%]
Thermal storage	30	200	95	10
Battery storage	150	530	95	10

Electrical and thermal load profiles, as well as the energy prices, are counted as three influential factors in the component sizing problem. In this paper, the average electricity and heat demand curves, generated solar PV and wind turbine power are utilised as depicted in Figs. 2 and 3.

Nonetheless, if the demand variations are significant for different days or seasons of a year, seasonal load classification or data clustering approach can be employed to estimate demands with an acceptable degree of certainty at a given day to reduce the optimisation horizon for the optimal cogeneration system sizing problem [42]. In this paper, the temporal horizon of the optimisation problem is 24 hours.

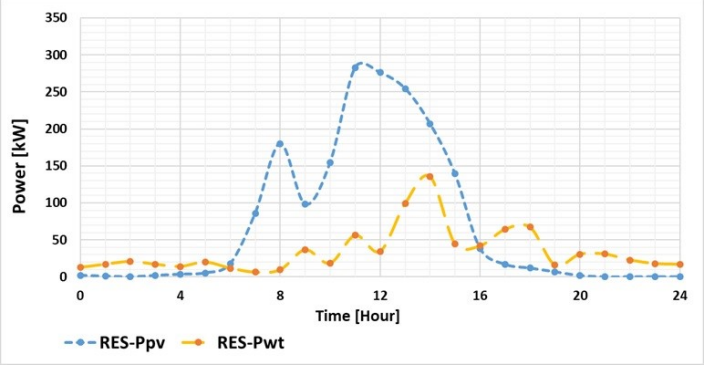

Figure 3. Renewables generation over the planning horizon

Considering the aforementioned technical and economic characteristics of the candidate elements, the first case scenario inspects the performance of the proposed approach when both ESDF and PFSI are neglected.

In this case, one CHP unit of type A (m_a) and one AB unit of type A (n_b) are required to meet the thermal and electrical load. Furthermore, utilising energy storage devices in the energy hub makes the system more economically viable as they store the generated surplus energy and inject this energy when it is financially beneficial. The BES stores the excess power generated by RESs or CHP units, whereas the thermal storage stores the cogenerated heat produced by the CHP devices. In this case, the optimal capacity and power of the TES are obtained at 416.35 kWh and 273.92 kW, respectively. The size of energy storage depends not only on the electricity and gas market prices but also the thermal and electricity load curves. Tables 4 and 5 represent the optimal configuration and size of the ESSs for the understudy cogeneration system in the defined case studies.

Table 4. Optimal configuration of the cogeneration system in different case scenarios

Cases	CHP	AB
A	$1 \times typeA + 0 \times typeB$	$1 \times typeA + 0 \times typeB$
B	$0 \times typeA + 1 \times typeB$	$1 \times typeA + 0 \times typeB$
C	$1 \times typeA + 0 \times typeB$	$1 \times typeA + 0 \times typeB$

In scenario B, the defined PFSI is considered in the developed model to alleviate the costs associated with grid power variations. However, the ESS degradation index is neglected. From the grid's perspective, wide fluctuations in the demand would destabilise the grid, incurring further operation costs to respond to the changes. Therefore, a proportion of this cost is imposed on the consumer to penalise the extreme demand fluctuations and encourage the consumers to regulate their importing power. As the defined PFI is implemented as a term in the main objective function with a pertaining weight, the grid fluctuations can be effectively reduced, proportional to the assigned weight as represented in Fig. 4. The figure on the left illustrates the impact of weight variation on the power purchased from the grid after performing the operation optimisation. In this figure, different colours denote various assigned PFSI weights. The figure on the right, however, shows the sensitivity of PFSI with respect to PFSI weight variations.

Table 5. Energy storage unit power and capacity rating for different case scenarios

Cases	A	B	C
BES PR [kW]	0	236.16	213.94
BES CR [kWh]	0	674.48	406.50
TES PR [kW]	273.92	220.31	211.44
TES CR [kWh]	416.35	446.27	444.17

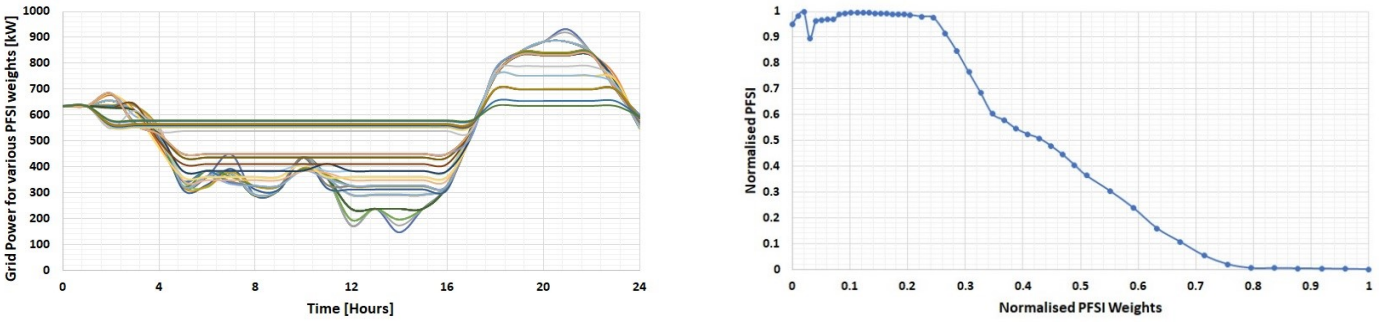

(a) (b)

Figure 4. Impact of PFSI on the purchasing power from the upstream grid: (a) Grid purchased power variations for different PFSI weights (b) Variations of PFSI index versus PFSI weight values

As described in Section 4, the planning of the cogeneration system is formulated as a multi-objective optimisation problem, constituting of multiple objectives including the defined PFSI. The cost associated with each objective determines the degree of importance of each individual object. In the case of PFSI, the attributed weight determines the degree of significance of PFSI the main objective function.

Analysing Fig. 4 (b), the variation of PFSI weight within 0 to 0.25 results in low sensitively of PFSI to PFSI weight and normalised PFSI of unity. Similarly, varying the PFSI weight values between 0.75 to 1, the PFSI will remain at 0, implicating a low sensitivity of PFSI to PFSI weight. However, the greatest sensitivity of PFSI to PFSI weight appears when the PFSI weight falls between 0.25 and 0.75. Within this range of PFSI weight, the normalised PFSI varies between 0 and 1. It should be noted that the normalised PFSI variation rate is higher in the lower side of 0.25-0.75 range.

Each curve represented in Fig. 4 (a) yields a data point illustrated in Fig. 4 (b). In Fig. 4 (a), the reflection of PFSI weights is represented on the grid power fluctuations. The grid power does not vary significantly over the first (0-0.25) and last range (0.75-1) of normalised PFSI weight as opposed to the middle range (0.25-0.75) where the peak demand is shaved and the deep valleys are filled.

The statistical analysis for grid fluctuations including the maximum and average grid power values versus variations of PFSI weight to reflect the importance degree of PFSI is obtained over the planning horizon as shown in Fig. 5. In this figure, the three distinct areas are identified as explained above. Within each region, the calculated value may vary within a limited range as calculated in Fig.5. As it is evident from Fig.5, the fluctuation range within the first and last regions for variations in both average grid power and max grid power is very small and do not exceed 2.2% at the highest due to the low sensitivity of PFSI in these regions. On the other hand, in the second region, the variations in the average grid power and max grid power parameters are comparatively wide (approximately 9% at the highest) due to the high sensitivity of the system within this range as previously described.

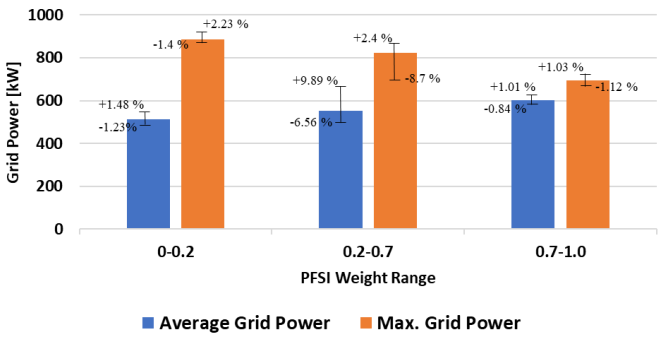

Figure 5. Statistical comparison of grid fluctuations parameters in three different variation regions of PFSI

In case C, both ESS degradation factor and grid fluctuations index are included in the objective function. Implementing the proposed MIQP approach, the optimal capacity and power rating for BES and TES are obtained 213.94 kW, 406.5 kWh, 211.44 kW, and 444.17 kWh, respectively which are less than the values calculated for scenario B. Comparing case B and C, it can be inferred that the impact of ESS degradation index is less compared to the PFSI. On the other hand, the optimal structure of the system is similar to case B except for the CHP unit type B that provides greater power compared to type A as its maximum power and ramp-up limit are greater. Although the efficiency of CHP type B is slightly less than type A, it is relatively more expensive. Therefore, due to the impact of ESS degradation on the optimal operation of the cogeneration system, the algorithm prefers to lessen the size of the BES and TES while increasing the size of CHP units.

In scenario C that the degradation of BES is modelled through associating an appropriate coefficient to the ESDF in the objective function, the ESS power and capacity ratings have decreased compared to the scenario B. It should be noted that the PFSI factor is considered in both the case B and C. The ESS depreciation index affects the optimal operation of conversion units to reduces the ESS power and capacity ratings as the extensive operation of ESS would not be economical unless it effectively lessens the electricity or gas cost.

The calculated optimal structure of the cogeneration system consists of one CHP unit of type A and one unit of type A (n_a) as stated in Table 4. The optimised configuration of the understudy system is demonstrated in Fig. 6. The TES parameters are also affected by including ESS depreciation factor (ESDF) due to the trade-off between ESSs associated costs and the costs of energy carriers at the input of CHP. As a result, the TES power and capacity are slightly decreased.

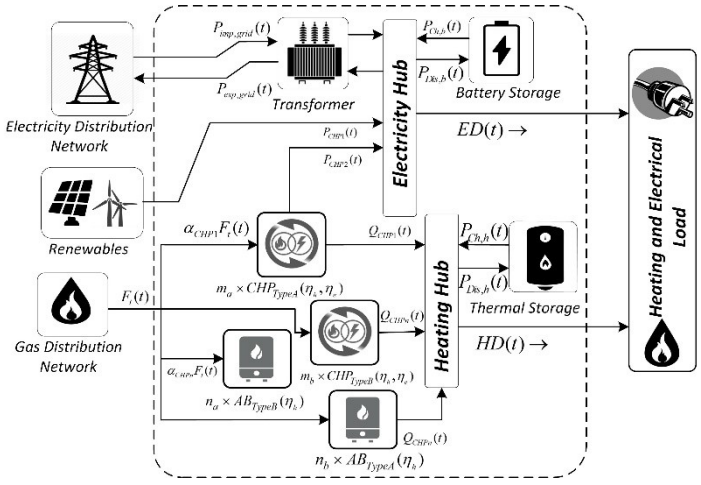

Figure 6. Structure of the optimised cogeneration system

Besides the size of ESSs, solving the unit commitment problem for each candidate solution ensures that the optimal solution will result in economic dispatching while satisfying the technical requirements. The optimal energy variations for BES and TES, and the power exchanged with the upstream grid which are achieved by addressing the unit-commitment problem for all three scenarios are demonstrated in Figs. 7 to 9, respectively.

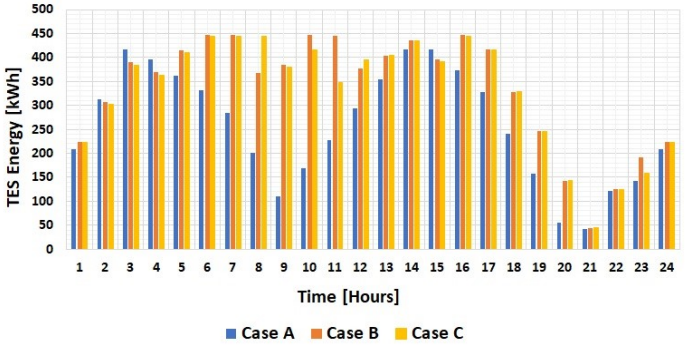

Figure 7. Optimal operation of thermal energy storage for different scenarios

The optimal operation of components depends on the cost of energy carriers, the PFSI, and degradation factor coefficients as well as heat and electricity load demands. The BES stores energy during the off-peak period and when the CHP converter is running to meet the thermal demand and deliver this energy over the peak period.

Considering PFSI in the optimisation model, a trade-off between the energy cost and power fluctuation range is established and hence affecting the operation of the ESSs devices as illustrated in Figs. 7 to 9. As it is clear from Table 4 and 5, considering the PFSI in the optimisation model and ignoring the depreciation factor substantially increases the size of the energy storage units, resulting in less investment on the energy conversion units.

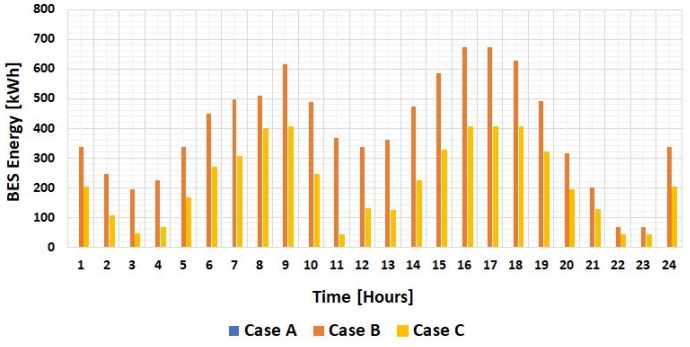

Figure 8. Optimal operation of battery energy storage for different scenarios

As demonstrated in Fig. 7, in case A where neither PFSI nor ESDF are included in the objective function, the stored energy in the TES follow the thermal and electricity demand patterns. If the peak period of thermal demand overlaps with that of electricity demand, the CHP unit along with the upstream grid contributes to the electricity load. However, due to high thermal demand, the output of the CHP unit increases to meet the thermal demand concurrently. The inclusion of PFSI objective in the optimisation model in case B leads to a substantial change in TES energy variation. The primary reason for this significant change is rooted in the change of CHP unit commitment duration and output power magnitude to mitigate the grid power fluctuations as represented in Fig. 9. These variations can be obviously observed in Fig. 8, wherein the BES is charged during the off-peak period and dispatched the stored energy during the high peak demand to minimise the PFSI for case B, in contrast to case A in which no BES is required.

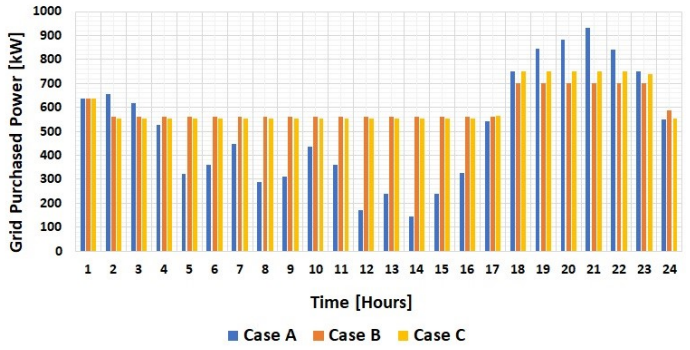

Figure 9. Grid operation for different scenarios

The impact of ESDF on the cogeneration system planning and

operation optimisation is revealed through implementing case C. Since the depreciation of the BES directly affects its operation and consequently, the commitment status of the other elements in the cogeneration system, the extensive usage of energy storage will increase the operation cost. Besides, as explained earlier, including the ESDF and PFSI in the objective function establishes a trade-off between the two performance indices. Hence, the BES capacity is lessened compared to case B and the operation of BES and TES is slightly changed during the valley and peak periods, causing the PFSI to increase. A similar pattern is obtained in grid operation as shown in Fig. 8.

6. Conclusion

This paper presented a MIQP based optimisation approach for sizing and scheduling of cogeneration systems, considering the degradation of battery energy storage as well as grid fluctuations. The proposed method solves a unit commitment problem to optimise the cogeneration system configuration while meeting the operating criteria of the candidate components. In order to take the BES degradation phenomena into account, the quadratic factor, ESDF is defined and included in the objective function, relating the sizing parameters to operating variables. Furthermore, the PFSI is introduced to reflect the variations of the grid power. Considering this index with appropriate weight in the objective function will optimally mitigate the grid fluctuations. To investigate the level of impact of PFSI and ESDF on the optimal structure of the cogeneration system, the developed model was implemented for three case studies. The obtained results confirmed the performance and applicability of the proposed approach for planners to optimally determine the structure of cogeneration systems.

References

[1] Ma T, Wu J, Hao L. Energy flow modelling and optimal operation analysis of the micro energy grid based on energy hub. Energy Convers Manag 2017;133:292–306. https://doi.org/10.1016/j.enconman.2016.12.011.

[2] Garmabdari R, Moghimi M, Yang F, Gray E, Lu J. Multi Energy System Modelling and Operation Optimisation for University Research Facility. Proc. - 2018 IEEE Int. Conf. Environ. Electr. Eng. 2018 IEEE Ind. Commer. Power Syst. Eur. EEEIC/I CPS Eur. 2018, 2018. https://doi.org/10.1109/EEEIC.2018.8494607.

[3] Mancarella P. MES (multi-energy systems): An overview of concepts and evaluation models. Energy 2014;65:1–17. https://doi.org/10.1016/j.energy.2013.10.041.

[4] Mohammadi M, Noorollahi Y, Mohammadi-ivatloo B, Yousefi H. Energy hub: From a model to a concept – A review. Renew Sustain Energy Rev 2017;80:1512–27. https://doi.org/10.1016/j.rser.2017.07.030.

[5] Maroufmashat A, Sattari S, Roshandel R, Fowler M, Elkamel A. Multi-objective Optimization for Design and Operation of Distributed Energy Systems through the Multi-energy Hub Network Approach. Ind Eng Chem Res 2016;55:8950–66. https://doi.org/10.1021/acs.iecr.6b01264.

[6] Fuentes-Cortés LF, Santibañez-Aguilar JE, Ponce-Ortega JM. Optimal design of residential cogeneration systems under uncertainty. Comput Chem Eng 2016;88:86–102. https://doi.org/10.1016/j.compchemeng.2016.02.008.

[7] Bianchi M, De Pascale A, Melino F. Performance analysis of an integrated CHP system with thermal and Electric Energy Storage for residential application. Appl Energy 2013;112:928–38. https://doi.org/10.1016/j.apenergy.2013.01.088.

[8] SoltaniNejad Farsangi A, Hadayeghparast S, Mehdinejad M, Shayanfar H. A novel stochastic energy management of a microgrid with various types of distributed energy resources in presence of demand response programs. Energy 2018;160:257–74. https://doi.org/10.1016/j.energy.2018.06.136.

[9] Fabrizio E. Modelling of multi-energy systems in buildings. Inst Natl Des Sci Appliquées Lyon 2008:170.

[10] Evins R, Orehounig K, Dorer V, Carmeliet J. New formulations of the "energy hub" model to address operational constraints. Energy 2014;73:387–98. https://doi.org/10.1016/j.energy.2014.06.029.

[11] Leadbetter J, Swan L. Battery storage system for residential electricity peak demand shaving. Energy Build 2012;55:685–92. https://doi.org/10.1016/j.enbuild.2012.09.035.

[12] Garmabdari R, Moghimi M, Yang F, Gray E, Lu J. Battery energy storage capacity optimisation for grid-connected microgrids with distributed generators. 2017 Australas Univ Power Eng Conf AUPEC 2017 2018;2017-Novem:1–6. https://doi.org/10.1109/AUPEC.2017.8282480.

[13] Zammit M. Managing Peak Demand 2005. http://www.energyresponse.com/uploads/managing peak demand by m zammit.pdf.

[14] Shahmohammadi A, Dalvand MM, Ghazizadeh MS, Salemnia A. Energy hubs' structural and operational linear optimization with energy storage elements. 2011 2nd Int. Conf. Electr. Power Energy Convers. Syst. EPECS 2011, 2011, p. 1–6. https://doi.org/10.1109/EPECS.2011.6126801.

[15] Fabrizio E, Corrado V, Filippi M. A model to design and optimize multi-energy systems in buildings at the design concept stage. Renew Energy 2010;35:644–55. https://doi.org/10.1016/j.renene.2009.08.012.

[16] Gabrielli P, Gazzani M, Martelli E, Mazzotti M. Corrigendum to "Optimal design of multi-energy systems with seasonal storage" [Appl. Energy (2017)]. Appl Energy 2018;212:720. https://doi.org/10.1016/j.apenergy.2017.12.070.

[17] Franco A, Bellina F. Methods for optimized design and management of CHP systems for district heating networks (DHN). Energy Convers Manag 2018;172:21–31. https://doi.org/10.1016/j.enconman.2018.07.009.

[18] Urbanucci L, Testi D. Optimal integrated sizing and operation of a CHP system with Monte Carlo risk analysis for long-term uncertainty in energy demands. Energy Convers Manag 2018;157:307–16. https://doi.org/10.1016/j.enconman.2017.12.008.

[19] Gamou S, Yokoyama R, Ito K. Optimal unit sizing of cogeneration systems in consideration of uncertain energy demands as continuous random variables. Fuel Energy Abstr 2003;44:116. https://doi.org/10.1016/s0140-6701(03)90896-4.

[20] Salimi M, Ghasemi H, Adelpour M, Vaez-ZAdeh S. Optimal planning of

energy hubs in interconnected energy systems: A case study for natural gas and electricity. IET Gener Transm Distrib 2015;9:695–707. https://doi.org/10.1049/iet-gtd.2014.0607.

[21] Bahlawan H, Morini M, Pinelli M, Spina PR. Dynamic programming based methodology for the optimization of the sizing and operation of hybrid energy plants. Appl Therm Eng 2019;160:113967. https://doi.org/10.1016/j.applthermaleng.2019.113967.

[22] Vahid A, Jadid S, Ehsan M. Optimal Planning of a Multi-Carrier Microgrid (MCMG) Considering Demand-Side Management. Int J Renew Energy Res 2018;8:238–49.

[23] Guo L, Liu W, Cai J, Hong B, Wang C. A two-stage optimal planning and design method for combined cooling, heat and power microgrid system. Energy Convers Manag 2013;74:433–45. https://doi.org/10.1016/j.enconman.2013.06.051.

[24] Amir V, Jadid S, Ehsan M. Optimal Design of a Multi-Carrier Microgrid (MCMG) considering net zero emission. Energies 2017;10:2109. https://doi.org/10.3390/en10122109.

[25] Pazouki S, Haghifam MR. Optimal planning and scheduling of energy hub in presence of wind, storage and demand response under uncertainty. Int J Electr Power Energy Syst 2016;80:219–39. https://doi.org/10.1016/j.ijepes.2016.01.044.

[26] Barbieri ES, Dai YJ, Morini M, Pinelli M, Spina PR, Sun P, et al. Optimal sizing of a multi-source energy plant for power heat and cooling generation. Appl Therm Eng 2014;71:736–50. https://doi.org/10.1016/j.applthermaleng.2013.11.022.

[27] Shao C, Wang X, Shahidehpour M, Wang X, Wang B. An MILP-Based Optimal Power Flow in Multicarrier Energy Systems. IEEE Trans Sustain Energy 2017;8:239–48. https://doi.org/10.1109/TSTE.2016.2595486.

[28] Buoro D, Casisi M, De Nardi A, Pinamonti P, Reini M. Multicriteria optimization of a distributed energy supply system for an industrial area. Proc 25th Int Conf Effic Cost, Optim Simul Energy Convers Syst Process ECOS 2012 2012;3:152–67.

[29] Shahmohammadi A, Moradi-Dalvand M, Ghasemi H, Ghazizadeh MS. Optimal Design of Multicarrier Energy Systems Considering Reliability Constraints. IEEE Trans Power Deliv 2015;30:878–86. https://doi.org/10.1109/TPWRD.2014.2365491.

[30] Pazouki S, Mohsenzadeh A, Ardalan S, Haghifam MR. Optimal place, size, and operation of combined heat and power in multi carrier energy networks considering network reliability, power loss, and voltage profile. IET Gener Transm Distrib 2016;10:1615–21. https://doi.org/10.1049/iet-gtd.2015.0888.

[31] Hussain A, Arif SM, Aslam M, Shah SDA. Optimal siting and sizing of tri-generation equipment for developing an autonomous community microgrid considering uncertainties. Sustain Cities Soc 2017;32:318–30. https://doi.org/10.1016/j.scs.2017.04.004.

[32] Catalina T, Virgone J, Blanco E. Multi-source energy systems analysis using a multi-criteria decision aid methodology. Renew Energy 2011;36:2245–52. https://doi.org/10.1016/j.renene.2011.01.011.

[33] Moghaddam IG, Saniei M, Mashhour E. A comprehensive model for self-scheduling an energy hub to supply cooling, heating and electrical demands of a building. Energy 2016;94:157–70. https://doi.org/10.1016/j.energy.2015.10.137.

[34] Yang H, Xiong T, Qiu J, Qiu D, Dong ZY. Optimal operation of DES/CCHP based regional multi-energy prosumer with demand response. Appl Energy 2016;167:353–65. https://doi.org/10.1016/j.apenergy.2015.11.022.

[35] Orehounig K, Evins R, Dorer V. Integration of decentralized energy systems in neighbourhoods using the energy hub approach. Appl Energy 2015;154:277–89. https://doi.org/10.1016/j.apenergy.2015.04.114.

[36] Maroufmashat A, Khavas SS, Bakhteeyar H. Design and Operation of a Multicarrier Energy System Based On Multi Objective Optimization Approach. Int J Environ Ecol Geol Geophys Eng 2014;8:590–5.

[37] Ramirez-Elizondo L, Velez V, Paap GC. A technique for unit commitment in multiple energy carrier systems with storage. 2010 9th Conf. Environ. Electr. Eng. EEEIC 2010, 2010, p. 106–9. https://doi.org/10.1109/EEEIC.2010.5489999.

[38] Beccuti G, Demiray T, Batic M, Tomasevic N, Vranes S. Energy hub modelling and optimisation: An analytical case-study. 2015 IEEE Eindhoven PowerTech, PowerTech 2015 2015. https://doi.org/10.1109/PTC.2015.7232413.

[39] Ren H, Gao W, Ruan Y. Optimal sizing for residential CHP system. Appl Therm Eng 2008;28:514–23. https://doi.org/10.1016/j.applthermaleng.2007.05.001.

[40] Garmabdari R, Moghimi M, Yang F, Gray E, Lu J. Multi-objective energy storage capacity optimisation considering Microgrid generation uncertainties. Int J Electr Power Energy Syst 2020;119:105908. https://doi.org/10.1016/j.ijepes.2020.105908.

[41] Morvaj B, Evins R, Carmeliet J. Optimization framework for distributed energy systems with integrated electrical grid constraints. Appl Energy 2016;171:296–313. https://doi.org/10.1016/j.apenergy.2016.03.090.

[42] Narimani A, Nourbakhsh G, Arefi A, Ledwich GF, Walker GR. SAIDI constrained economic planning and utilization of central storage in rural distribution networks. IEEE Syst J 2019;13:842–53. https://doi.org/10.1109/JSYST.2018.2852630.